Geophysical Research Letters

RESEARCH LETTER
10.1029/2023GL107561

Evolution of Antarctic Sea Ice Ahead of the Record Low Annual Maximum Extent in September 2023

Babula Jena[1], S. Kshitija[1], C. C. Bajish[2], John Turner[3], Caroline Holmes[3], Jeremy Wilkinson[3], Rahul Mohan[1], and M. Thamban[1]

[1]National Centre for Polar and Ocean Research, Ministry of Earth Sciences, Vasco da Gama, India, [2]KSCSTE-Institute for Climate Change Studies, Kottayam, India, [3]British Antarctic Survey, Natural Environment Research Council, Cambridge, UK

Key Points:

- The 2023 Antarctic sea ice extent maximum on 7 September (16.98×10^6 km^2) was the lowest annual maximum in the satellite era
- Anomalous upper-ocean warming and strong northerly winds contributed to impeding the ice expansion in the Ross and Weddell Seas
- Quasi-stationary and explosive polar cyclones contributed to periods of southward ice-edge shift in both sectors

Supporting Information:

Supporting Information may be found in the online version of this article.

Correspondence to:

B. Jena,
bjena@ncpor.res.in

Citation:

Jena, B., Kshitija, S., Bajish, C. C., Turner, J., Holmes, C., Wilkinson, J., et al. (2024). Evolution of Antarctic sea ice ahead of the record low annual maximum extent in September 2023. *Geophysical Research Letters*, *51*, e2023GL107561. https://doi.org/10.1029/2023GL107561

Received 30 NOV 2023
Accepted 11 MAR 2024

Author Contributions:

Conceptualization: Babula Jena
Formal analysis: Babula Jena, S. Kshitija, C. C. Bajish, John Turner, Caroline Holmes, Jeremy Wilkinson
Funding acquisition: Jeremy Wilkinson, Rahul Mohan, M. Thamban
Investigation: Babula Jena, S. Kshitija, Caroline Holmes, Jeremy Wilkinson
Methodology: Babula Jena, John Turner, Caroline Holmes
Project administration: Rahul Mohan, M. Thamban
Software: Babula Jena, S. Kshitija, C. C. Bajish
Visualization: Babula Jena, S. Kshitija, C. C. Bajish
Writing – original draft: Babula Jena

Abstract The 2023 Antarctic sea ice extent (SIE) maximum on 7 September was the lowest annual maximum in the satellite era (16.98×10^6 km^2), with the largest contributions to the anomaly coming from the Ross (37.7%, -0.57×10^6 km^2) and Weddell (32.9%, -0.49×10^6 km^2) Seas. The SIE was low due to anomalously warm (>0.3°C) upper-ocean temperatures combined with anomalously strong northerly winds impeding the ice advance during the fall and winter. Northerly winds of >12 ms^{-1} in the Weddell Sea occurred because of negative pressure anomalies over the Antarctic Peninsula, while those in the Ross Sea were associated with extreme blocking episodes off the Ross Ice Shelf. The Ross Sea experienced an unprecedented SIE decrease of -1.08×10^3 km^2 d^{-1} from 1 June till the annual maximum. The passage of quasi-stationary and explosive polar cyclones contributed to periods of southward ice-edge shift in both sectors.

Plain Language Summary Sea ice provides a vital habitat for life in the Southern Ocean, and plays an important role in the ocean circulation, the dynamics of the Earth's climate, the biogeochemical cycle, and the regional ecosystem. Climatologically, Antarctic sea ice expands northwards from the continent each autumn and winter. However, in 2023 an unprecedented slow ice expansion occurred in the Southern Ocean ahead of the annual maximum on 7 September of 16.98×10^6 km^2, which was 1.46×10^6 km^2 below the long-term average. In fact, the area covered by ice remained at a record low level every day from 21 April 2023 until 11 November 2023. Our findings suggest that an impact of upper-ocean warming and changes in winds, combined with heat and moisture fluxes, extreme winds and high ocean waves associated with polar cyclones (storms), contributed to these record low ice conditions. In particular, cyclones caused episodes of exceptional slow ice expansion or even retreat, leading to negative ice anomalies. For instance, the ice-edge in the Weddell Sea was moved southwards quickly in a few days (up to 256 km southward) with an ice area loss of $\sim 2.3 \times 10^5$ km^2, equivalent to the size of United Kingdom.

1. Introduction

During the satellite-era starting in 1978, the Southern Ocean sea ice extent (SIE) moderately increased until 2015, followed by a decrease from 2016 to 2023 (Purich & Doddridge, 2023) (Figure 1a). The overall expansion of SIE in the Southern Ocean has been attributed to a variety of physical drivers (Bintanja et al., 2013; Doddridge & Marshall, 2017; Fogt et al., 2022; Haumann et al., 2016; Holland et al., 2017). Following the moderate increase in SIE, a rapid decrease took place in summer 2016/17, associated with a negative phase of Southern Annular Mode (SAM) with weakened westerlies, deepening of the Amundsen Sea Low (ASL), intensification of atmospheric zonal wave three (Schlosser et al., 2018), passage of anomalous polar storms (Turner et al., 2017; Wang et al., 2019), persistence of El-Nino-induced warm water (Stuecker et al., 2017), and a record strength in the negative phase of the Indian Ocean dipole and La Niña (Purich et al., 2022; Wang et al., 2019). From 2007 to 2021, it has been difficult to explain the influence of SAM on low SIE because of the strengthening in the non-annular structure of SAM (Schroeter et al., 2023). It has been found that periods of large negative SIE anomalies during the ice growth season, were following the passage of explosive polar cyclones (Jena et al., 2022; Vichi et al., 2019). After the 2016/17 event, the Southern Ocean ice extent reached another record low in summer 2021/22 as a result of the combined influences of a strengthening of ASL, a positive SAM, polar cyclones, and opening of an extensive polynya in the Ross Sea (Turner et al., 2022).

The change in depth and location of the ASL strongly influences the SIE in the Ross Sea, Weddell Sea and Amundsen-Bellingshausen Seas (ABS) (Hosking et al., 2013). The ASL has a large locally driven internal climate

Writing – review & editing: Babula Jena, S. Kshitija, C. C. Bajish, John Turner, Caroline Holmes, Jeremy Wilkinson, Rahul Mohan, M. Thamban

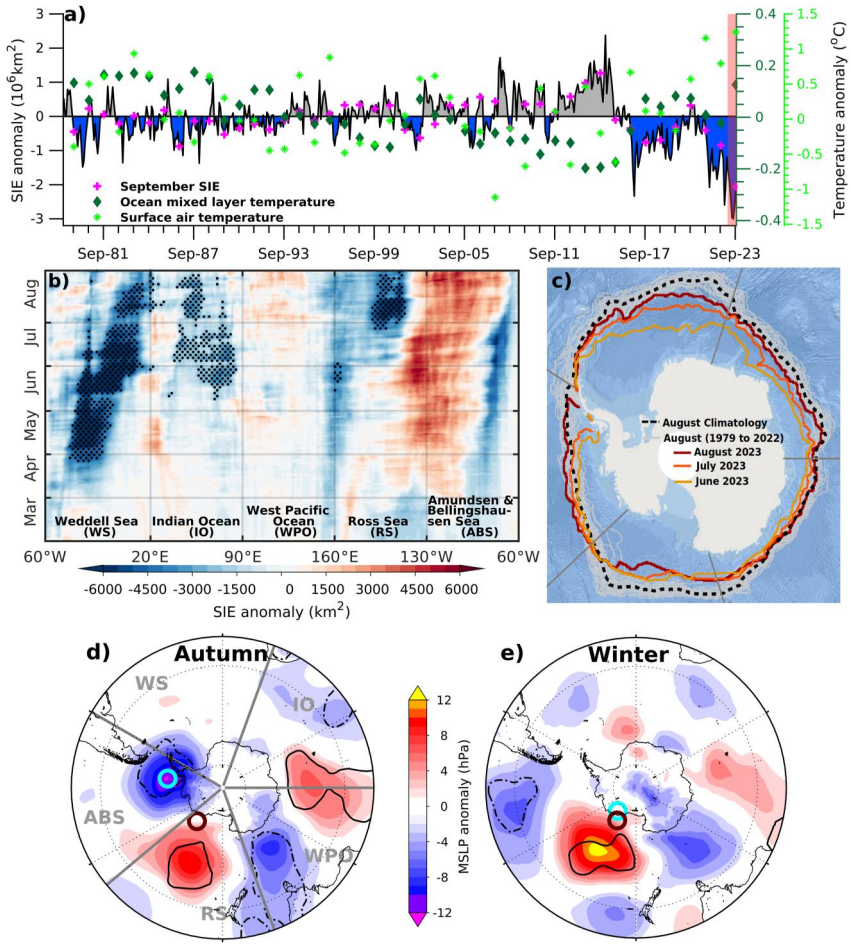

Figure 1. (a) Monthly sea ice extent (SIE) anomalies for the Southern Ocean, with the points representing September SIE and ocean–atmospheric temperature (55°S–75°S). The SIE anomaly during March–September 2023 is highlighted in red. (b) Sector-wise evolution of SIE anomaly in 0.2° longitude, with the dots indicating record low values. (c) The unprecedented low SIE in winter 2023, except for ice expansion in the much of the Amundsen-Bellingshausen Seas sector. The most pronounced poleward shift of the ice-edge is evident in the Weddell and Ross Seas. (d)–(e) Mean sea level pressure (MSLP) anomaly for 2023. Regions inside dashed (solid) black-polylines have record low (high) MSLP. The cyan and brown circles show the location of Amundsen Sea Low (Hosking et al., 2013) for 2023 and the climatological mean, respectively.

variability and is modulated by the El Niño Southern Oscillation (ENSO) and the SAM (Li et al., 2021; Turner et al., 2015). Also, enhanced atmospheric blocking strongly influences the surface climate variability over the Ross Sea, Weddell Sea, and ABS region through its meridional flow component (Emanuelsson et al., 2018). It is therefore clear that a change in the synoptic environment can impact the SIE conditions.

Recently, a record low SIE was established in summer 2022/23, partially linked to decadal warming of the Southern Ocean (Purich & Doddridge, 2023) (Figure 1a). The SIE in its growth period usually remains within ±2 standard deviations from the long-term mean even after exceptionally low SIE events including summer of 2016/2017 and 2021/2022 (Figure S1a in Supporting Information S1). However, an unprecedented slow ice expansion occurred ahead of the annual maximum in 2023 (exceeding four standard deviations below the long-term mean), in a background of anomalously warm ocean-atmospheric conditions (Figure 1a, Figure S1a in Supporting Information S1). The SIE was at a record low level every day from 21 April to 11 November and reached an early annual maximum on 7 September 2023. Three of the five sectors around Antarctica also experienced record low annual maxima, although on different dates (Figure S1b in Supporting Information S1). In this paper, we investigate the exceptionally low SIE from March to September 2023 at a critical time of sea ice growth in its annual cycle (Figure 1a, Figure S1a in Supporting Information S1). We assess the role of large-scale atmospheric circulation anomalies, polar cyclones, and upper-ocean physical factors leading to record low SIE at an annual maximum.

2. Data and Methods

We utilized the observations of sea ice concentration (SIC) and SIE from the passive microwave satellite sensors that provided consistent and reliable data from 1979, with a spatial resolution of 25 km × 25 km (Fetterer et al., 2017). This product is generated using the NASA Team algorithm; for the latest observations, the near real time data are used (Meier et al., 2021). The SIE was calculated by summing up the pixel areas with a SIC of 15% or greater. The anomaly was computed with reference to the long-term mean from 1979 to 2008. Sea ice velocity was calculated from wind vectors (ECMWF ERA5) using a standard methodology (Campbell et al., 2019; Martinson & Wamser, 1990).

In order to characterize the atmospheric circulation, the ECMWF ERA5 product was used at a grid resolution of 0.25° × 0.25° (Hersbach et al., 2023). The net heat flux (NHF) was computed by summing the shortwave radiation, outgoing long-wave radiation, sensible and latent heat flux. The positive (negative) values of NHF show heat gain (loss) by the ocean surface. We generated the six hourly cyclone track and categorized each cyclone for the WC (Weddell Sea cyclone) and RC (Ross Sea cyclone), using an established method (Jena et al., 2022; Xia et al., 2012). The explosive events were characterized when the normalized deepening rate (NDR_r) of relative central pressure exceeded unity within 24 hr. Quality-controlled potential temperature and salinity data at a grid spacing of 0.25° × 0.25° was used from ECMWF ORAS5 (Zuo et al., 2019). The mixed layer depth was calculated as the depth where the upper-ocean potential density changes by 0.01 kg m^{-3} in comparison to the surface (Kaufman et al., 2014). References to record values, for all oceanic and atmospheric variables, refer to a record for the satellite era 1979–2023. The SAM index was acquired from https://legacy.bas.ac.uk/met/gjma/sam.html (Marshall, 2003) and Niño 3.4 anomalies from https://psl.noaa.gov/gcos_wgsp/Timeseries/Nino34/ (Rayner et al., 2003).

3. Climatological Factors Influencing Ice Growth Ahead of the Annual Maximum

Climatologically the Antarctic SIE expands from an annual minimum of 2.85 × 10^6 km^2 on 20 February to a maximum of 18.62 × 10^6 km^2 on 21 September through the ice growth period from March to September (Figure S1a in Supporting Information S1). At this annual maximum, most of the sea ice is found in the Weddell Sea (36%, 6.68 × 10^6 km^2), followed by the Ross Sea (22%, 4.1 × 10^6 km^2), Indian Ocean sector (IO, 19.7%, 3.67 × 10^6 km^2), ABS (11.8%, 2.21 × 10^6 km^2), and West Pacific Ocean (WPO) sector (10.3%, 1.92 × 10^6 km^2). Ahead of the annual maximum, the daily rate of sea ice growth is largest in May (Table S1 in Supporting Information S1).

To examine the atmospheric circulation anomalies linked with low SIE during the annual maximum, we analyzed the difference in mean sea level pressure (MSLP) by subtracting the upper quartile of years from the lower quartiles of annual maximum SIE years (Figure S2 in Supporting Information S1). We have considered the composite of MSLP for ice growth seasons, specifically austral Fall (March to May) and winter (June to August) prior to the annual maximum. The composite analysis of MSLP for the Weddell Sea SIE indicates the significant strengthening of the ASL and its eastward shift relative to its mean position in both autumn and winter, ahead of a low SIE at the maximum (Figure S2 in Supporting Information S1). The presence of the ASL and an anticyclone over the South Atlantic Ocean promote the strengthening of northerly winds across the Weddell Sea. This strong onshore flow, along with warm air advection, pushes the ice-edge southward, contributing to the low ice extent in the Weddell Sea. Analysis of the conditions in the Ross Sea shows the development of a significantly high MSLP anomaly (atmospheric blocking high) near 130°W and a low-pressure area to its west during autumn–winter, preceding the occurrence of low SIE at an annual maximum. This pressure pattern gives strong northerly winds into the Ross Sea, contributing to low SIE in the region.

Therefore, the composite analysis shows that the strengthening and eastward shifting of the ASL is important ahead of low SIE at an annual maximum for the Weddell Sea. Furthermore, the development of an atmospheric block near 130°W appears to be important for the Ross Sea.

4. Reduced Ice Expansion Ahead of the 2023 Annual Maximum

4.1. Regional SIE Anomalies in the Southern Ocean

The daily evolution of SIE anomalies by longitude ahead of the annual maximum 2023 is illustrated in Figure 1b. In summer 2023, the entire Southern Ocean experienced a record low SIE (1.76 × 10^6 km^2) on 19 February and

was essentially ice-free by this month, except for a large area of multiyear ice in the Weddell Sea that followed the climatological ice–edge (Figure S3 in Supporting Information S1).

During the onset of ice growth in March 2023, a region of negative sea ice anomalies developed to the east of the Antarctic Peninsula in the western Weddell Sea (Figure 1b). These negative anomalies extended eastward and remained a persistent feature from April to September 2023, with record low SIE initiated from 21 April that continued till the annual ice maximum. The negative anomalies observed in April were further enhanced to an even larger anomaly in May that translated zonally toward the Lazarev Sea (east of the prime meridian) from June to September. The SIE anomalies in the Weddell Sea during the ice growth phase of 2023 was one of the most long-lived record anomalies observed in the satellite era since 1979 (Figure S4a in Supporting Information S1).

Negative ice anomalies persisted in the eastern WPO from March to September 2023 (Figure 1b). This anomalous feature progressed eastward to the part of Ross Sea, extending to 175°E from late April to June. From July onwards, the region of negative ice anomalies extended eastward over a wider region of the Ross Sea (up to 145° W) that continued till September. The Ross Sea experienced record-low SIE every day from 27 July to 6 September 2023 (Figures 1b and 3a). In contrast, a positive ice anomaly was present over parts of the eastern Ross Sea and the entire Amundsen Sea from April to September 2023. In the Bellingshausen Sea, east of the Amundsen Sea and west of the peninsula, large negative anomalies in much of the ice growth season gradually gave way to mostly positive anomalies by the winter maximum (Figures 1b and 1c) (Gilbert & Holmes, 2024). A negative anomaly also developed in the Indian Ocean with record low SIE from 18 June to 1 September (Figure 1b, Figure S1b in Supporting Information S1).

On 7 September 2023, the Southern Ocean experienced a new record low SIE (16.98×10^6 km^2) at an annual maximum in the satellite era, which was 1.46×10^6 km^2 below the climatological mean (Figure S1a in Supporting Information S1). By this date all sectors except the ABS had record negative SIE anomalies, with the largest contributions from the Ross (37.7%, anomaly of -0.57×10^6 km^2) and Weddell (32.9%, -0.49×10^6 km^2) Seas, followed by the IO (21.6%, -0.32×10^6 km^2) and WPO (2.3%, -0.03×10^6 km^2) (Figure S4b in Supporting Information S1). Ahead of the annual maximum, the largest contribution to the negative anomaly came from the Weddell Sea from April to July (43.7%–57.6%), maximum being in May (Figure S3 in Supporting Information S1). After that, in August and September, the Ross Sea contribution dominated (44.4%–47.3%), followed by the Weddell Sea (39.2%–42%). This suggests that the Weddell and Ross Seas contributed most to the slowdown in ice expansion ahead of the record low hemispheric annual maximum. In autumn, the reduced ice expansion was largest in the Weddell Sea (20.7×10^3 km^2 d^{-1}), being 39.3% less than the mean rate (Table S1 in Supporting Information S1). In winter, the reduced ice expansion was largest in the Ross Sea with a most rapid rate of -1.08×10^3 km^2 d^{-1}, which was 110% slower than the mean rate.

4.2. The Weddell Sea

The evolution of the ocean mixed layer temperature (MLT) based on reanalysis data showed an anomalous warming (>0.5°C) in the Weddell Sea from late 2016 to winter 2023 (Figure S5 in Supporting Information S1). Similar ocean warming features were also observed using Argo observations (Purich & Doddridge, 2023). The persistent warm anomalies over seven years and the presence of anomalously warm water near the ice-edge in 2023 (Figures S5 and S6 in Supporting Information S1) suggested the importance of ocean preconditioning to the negative SIE anomaly. Moreover, the atmosphere also played a key role in accounting for the low SIE.

In autumn 2023, the atmospheric circulation anomaly was characterized by a positive SAM (index 0.74) and deepening of the ASL (anomaly > 12 hPa) with record negative pressure anomalies over a large area covering both the Bellingshausen and western Weddell Seas (Figure 1d). The ASL was located consistently close to the western Antarctic Peninsula experiencing an eastward shift from its mean position. From March to April, to the east of the ASL, there was atmospheric blocking over the Lazarev Sea near the prime meridian (Figure S6 in Supporting Information S1). The ASL was particularly deep in May (anomaly > 16 hPa), exceeding 3 standard deviations from the long-term mean, associated with a prominent pattern of atmospheric zonal wave three. The strengthening of the ASL and its persistent eastward location resulted in anomalous northerly flow with monthly winds exceeding 12 ms^{-1} across the Weddell Sea. The northerly wind advected heat flux from mid-latitudes into the region, resulting in record anomalous warming (>13°C) of surface air temperature (SAT) over the Weddell Sea, particularly in April and May (Figure S6 in Supporting Information S1). The MLT was at a record high level

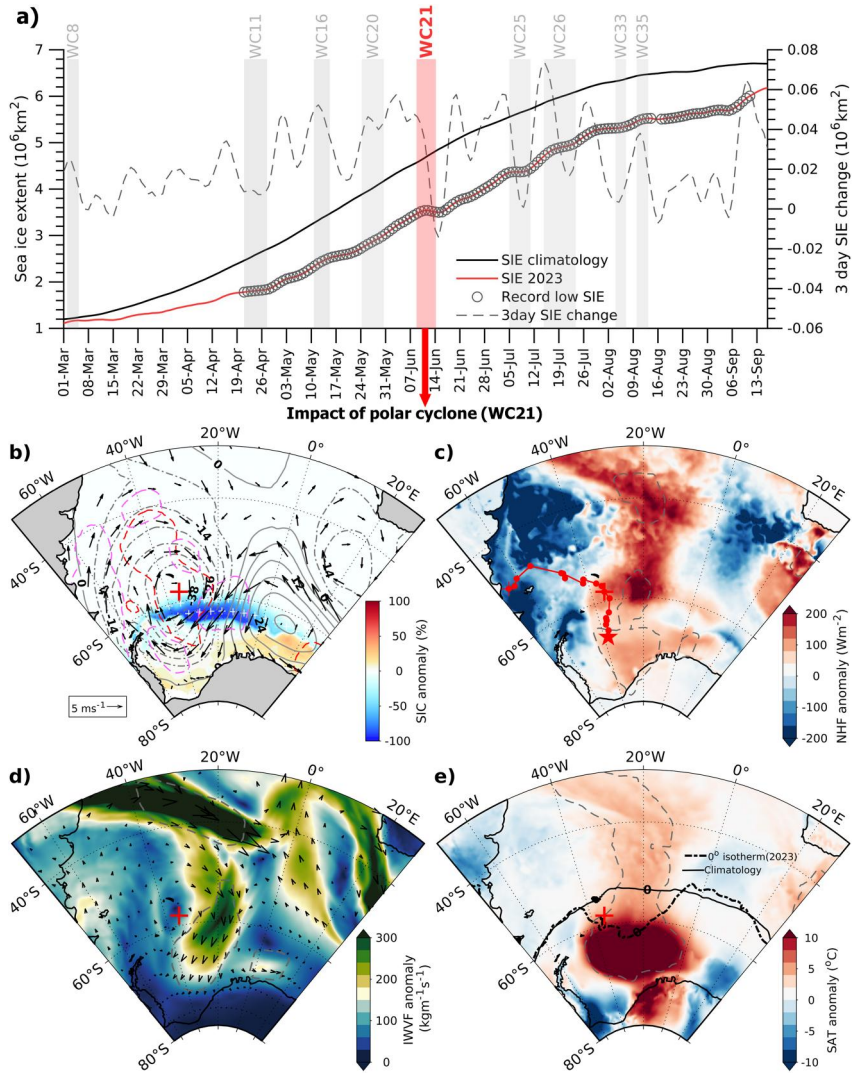

Figure 2. Sea ice evolution in the Weddell Sea (60°W–20°E) and its association with cyclones. (a) The daily sea ice extent (SIE) from 1 March to annual ice maximum 2023, along with the record low values (circle), 3-day change, and climatological SIE. Bars indicate the occurrence of Weddell Sea cyclones (WC) corresponding to the 3-day slowest ice expansion or retreat. The cyclone numbers and tracks are shown in Figure S7 in Supporting Information S1. The largest ice retreat took place following the passage of a poleward-moving quasi-stationary cyclone (WC21, red-shaded bar). The passage of WC21 with the anomalies of (b) sea ice concentration (SIC), mean sea level pressure (MSLP) (positive and negative anomalies are shown in solid and dot-dashed gray contours, respectively), 10 m wind (black arrow), (c) net heat flux (NHF), (d) integrated water vapor flux (IWVF), and (e) surface air temperature (SAT) with 0° isotherm on 11 June 2023 and climatology. In panel (b), red (magenta) contours represent record values for MSLP (wind). The white plus marks show record SIC anomalies. The WC21 track (red line, panel c) with its center on 11 June is shown in red plus mark. Gray contours (panels c–e) show record values for NHF, IWVF, and SAT.

with a temperature anomaly of more than 0.3°C. The findings suggest that ocean-atmospheric warming along with strong northerly winds contributed to the negative ice anomalies mainly near the marginal ice zone (MIZ). The Weddell Sea SIE was the10th lowest during March and the lowest ever extent in April (1.7×10^6 km^2) and May (2.5×10^6 km^2) which was 27.9–28.9% below the long-term mean (Figure S3 in Supporting Information S1). The contribution of negative anomaly increased from March (18.5%) to May (57.7%) due to strong northerlies associated with the ASL.

We highlight how transient weather systems in the Weddell Sea are important for SIE evolution in this period. We focus on the periods of slow ice expansion or retreat (Figure 2a), which corresponds to rapid amplification of the negative SIE anomaly. The March 3-day slowest ice expansion occurred from 3 to 15 March 2023, following the

passage of a series of cyclones, specifically an explosive development (WC8) that had extreme winds exceeding 22 ms^{-1} along the cyclone track (Figure 2a, Figure S7a in Supporting Information S1). The April 3-day slowest ice expansion took place following a poleward moving cyclone WC11 (20–27 April). In May, the slowest ice expansion occurred from 13 to 21 May, following an explosive system WC16 which developed within an extremely deepened ASL over the Bellingshausen Sea. This synoptic system followed an eastward trajectory along ~69°S covering the entire Weddell and Lazarev Seas. The system deepened to a record minimum central pressure of 931.5 hPa (anomaly, −53.8 hPa) at 18 UTC 12 May, with record winds exceeding 24 ms^{-1} (Figure not shown). The strong northerly flow with extreme ocean–atmospheric conditions during the cyclones contributed to a large negative SIE anomaly.

In June 2023, the atmospheric circulation changed with slightly negative pressure anomalies over the Weddell Sea accompanied by positive anomalies to its east along the prime meridian, which led to northerly flow into the eastern Weddell Sea (Figure S6 in Supporting Information S1). The negative SIE anomalies prevailed in June, particularly a sudden drop on 15 June with an ice retreat of -14.36×10^3 km^2 (Figure 2a) following the development of a quasi-stationary cyclone WC21 (8–14 June); this was the largest 3-day retreat in the 2023 ice growth season. This system initially followed a poleward trajectory, subsequently remaining quasi-stationary over the Weddell Sea ice cover from 10 to 14 June (Figure 2b). The system deepened with a minimum central pressure of 946.5 hPa (anomaly, −48.2 hPa). The record negative MSLP anomaly along the cyclone track was accompanied by a record positive MSLP anomaly (~33 hPa) to the east (Figure 2b). This pressure pattern gave a record strength of northerly winds with poleward advection of anomalous heat (>250 W m^{-2}) and moisture (>300 kg $m^{-1}s^{-1}$) flux along with an atmospheric river from the South Atlantic Ocean into the Weddell Sea (Figures 2b–2e, Figure S8a in Supporting Information S1); atmospheric rivers have previously been shown to be important for Weddell Sea ice variability in winter (Francis et al., 2020). The Weddell Sea experienced a record anomalous SAT increase of 18°C with the 0°C isotherm extending southwards to 68°S, allowing surface ice melt (Figure 2e). In parallel, intense winds (>20.6 ms^{-1} at 06 UTC 11 June) caused the formation of record significant wave height (SWH) of ~5.9 m (anomaly, 4.1 m) that propagated along the ice-edge (Figure S8b in Supporting Information S1). The ice-edge was moved southward by ~256 km (ice-cover loss of 0.23×10^6 km^2) from 9 to 15 June 2023 with an ice drift of ~0.56 ms^{-1}, following the passage of WC21 (Figure S9a in Supporting Information S1).

In July 2023, a negative MSLP anomaly remained over the Weddell Sea with a positive pressure anomaly to its north to northeast, resulting in monthly mean northerly winds of record strength across the eastern Weddell Sea, contributing to the negative ice anomaly (Figures S6 and S10 in Supporting Information S1). Two major events of slow ice expansion occurred, corresponding to the passage of one quasi-stationary cyclone WC25 followed by an explosive event WC26 (Figure 2a). In August 2023, a record meridional wind anomalies (>4.7 ms^{-1}) persisted across the Weddell Sea that arose from negative (positive) pressure anomaly over the western (eastern) Weddell Sea (Figures S6, S10 in Supporting Information S1). Two major episodes of 3-day slow ice expansion (-7.07×10^3 km^2) occurred during 4–8 August and 11–16 August as a result of the explosive cyclones WC33 and WC35, respectively (Figure 2a). It's worth noting that not all episodes of slow ice expansion or ice retreat can be attributed to cyclones, as other factors may also play a role.

In summary, during March–August 2023, several episodes of slow ice expansion or retreat took place in the Weddell Sea from the influence of anomalous ocean-atmospheric warming, deep ASL in autumn, strong northerly winds, and passage of 35 cyclones induced dynamic and thermodynamic factors. Ahead of the annual maximum, the Weddell Sea SIE reached its lowest ever extent in winter ($3.6–5.5 \times 10^6$ km^2), 14.4%–25.2% below the long-term mean (Figure S3 in Supporting Information S1).

4.3. The Ross Sea

During March 2023, a couplet of large positive (atmospheric blocking) and negative pressure anomalies developed over the Ross Sea (~135°W) and the eastern WPO, respectively (Figure S6a in Supporting Information S1). This pressure pattern directed northerly winds of record strength across the Ross Sea, with the peak wind speed exceeding 12 ms^{-1} over a large area. The strong northerly flow brought warm air from the southwest Pacific Ocean that contributed to reducing the ice expansion in the region. In particular, near ice-free conditions prevailed in the eastern Ross Sea (145°W–130°W) and the western Ross Sea (~160°E), corresponding to the anomalous warming of SAT (>4°C) and an area of warm water (MLT anomaly > 1.5°C) in March (Figures S3d

and S6a in Supporting Information S1). These conditions contributed to the negative ice anomalies in the Ross Sea, which were the ninth lowest March SIE (0.76×10^6 km^2), 37.3% below the climatological mean. In April 2023, high pressure anomalies over the Ross Sea and low over the WPO resulted in a northerly (southerly) flow into the western (eastern) Ross Sea, leading to a negative (positive) SIC anomaly within the Ross Sea (Figure S6b in Supporting Information S1).

During May and June, there was the development of a blocking high (centered at 160°W, between ~180°W and ~130°W) with record MSLP anomaly (>14 hPa) accompanied by the record negative anomaly (<12 hPa) over the WPO (120°E–160°E) (Figures S6c and S6d in Supporting Information S1). The pressure variability gave record strength northerly (southerly) flow into the western Ross Sea (Amundsen and eastern Ross Seas), reflecting a dipole pattern of warmer and colder SAT anomalies in the respective regions. These conditions caused negative SIC anomalies mainly in the MIZ of the western Ross Sea and more extensive ice than usual in the eastern Ross and Amundsen Seas. There were positive SIC anomalies in the southern part of the Ross Sea because of the strong northerly winds that pushed the ice southward, resulting in ice compaction.

From June to July, with a decaying ASL, the atmospheric circulation pattern changed dramatically with an eastward shift of the blocking high (centered at 130°W, between ~170°W and ~90°W) off the Getz Ice Shelf, along with large negative MSLP anomalies extending from the southwest Pacific Ocean to the WPO (Figure 1e, Figure S6e in Supporting Information S1). As a result, strong northerly flow with record meridional wind anomalies across the Ross Sea led to record SAT warming (anomaly > 10°C) over the entire region with a rapid eastward progression of negative SIC anomalies in July (Figure 1b, Figures S6 and S10 in Supporting Information S1). Furthermore, the Ross Sea exhibited anomalous warming of the MLT (~2.6°C) and anomalously warm water along the ice-edge was favorable for a reduced ice expansion (Figure S6 in Supporting Information S1). The Ross Sea SIE was the third lowest in July, 3.20×10^6 km^2 (Figure S3 in Supporting Information S1).

As for the Weddell Sea, we investigate the role of cyclones in the SIE evolution of Ross Sea. A large 3-day ice retreat occurred in early July 2023 (Figure 3a), peaking at -38.14×10^3 km^2 on 4 July, following the passage of a poleward moving quasi-stationary explosive cyclone RC24 (28 June–04 July 2023). This synoptic system formed east of New Zealand at 18 UTC 28 June and developed into an explosive event at 00 UTC 30 June that followed a southward trajectory near ~180°E (Figure 3b). The system deepened to a minimum central pressure of 944.9 hPa (anomaly, −53.9 hPa) with a maximum wind speed of 30.5 ms^{-1} at 06 UTC 01 July, and it remained quasi-stationary from 01 to 04 July. A record negative pressure anomaly along the cyclone track was accompanied by a record positive pressure anomaly (>30 hPa) to its east, giving strong northerly winds across the Ross Sea (Figure 3b). The northerly flow was associated with a feature that resembled an atmospheric river carrying anomalous heat (>207 W m^{-2}) and moisture-laden airmass (integrated water vapor flux > 420 kg m^{-1}s^{-1}) along with a cloud band stretching from the South Pacific Ocean to the Ross Sea (Figures 3b–3e, Figure S8c in Supporting Information S1). An anomalous atmospheric warming of up to ~20°C was observed with the 0°C isotherm reaching poleward to 72°S (between 180°W and 140°W), impeding the ice expansion mainly in the MIZ during the cyclone episode (Figure 3e). In parallel, the intense winds during the cyclone RC24 led to the formation of large ocean waves with SWH up to 7.5 m (anomaly, 2.8 m), which propagated toward the MIZ, providing sufficient energy to mechanically break the ice (Jena et al., 2022; Vichi et al., 2019) (Figure S8d in Supporting Information S1). The strong northerly winds moved the ice-edge southward with an ice drift of ~0.65 ms^{-1}, thereby retreating the ice-edge by ~131 km (ice-cover loss of 0.25×10^6 km^2) from 30 June to 04 July (Figure S9b in Supporting Information S1). Similarly, a consistent decline in SIE took place from 20 to 28 July due to the combined influence of extreme ocean–atmospheric conditions associated with a series of four polar cyclones (RC25–RC28) (Figure S7b in Supporting Information S1).

During August, the atmospheric blocking intensified to a record high pressure (anomaly > 14 hPa) to the north of Ross Ice Shelf, accompanied by a negative anomaly to its west that gave record northerly (southerly) flow into the entire Ross Sea (ABS) (Figure S6f in Supporting Information S1). The flow led to a dipole pattern with record temperature anomaly (>9°C) in the Ross Sea and cold air outbreaks from the interior of Antarctica into the ABS sector. These conditions resulted in negative SIC anomalies in the Ross Sea and more extensive ice in the ABS, reflecting an east-west dipole pattern. By August, sea ice was expansive throughout the ABS but earlier, as late as June, there was virtually no sea ice in the Bellingshausen (Figure 1c), consistent with northerlies associated with a decaying ASL. The region of maximum ice-edge retreat in the Ross Sea (180°W to 140°W) was collocated closely with the region of record northerly winds reaching 12 ms^{-1} (Figure S6f in Supporting Information S1). In

10.1029/2023GL107561

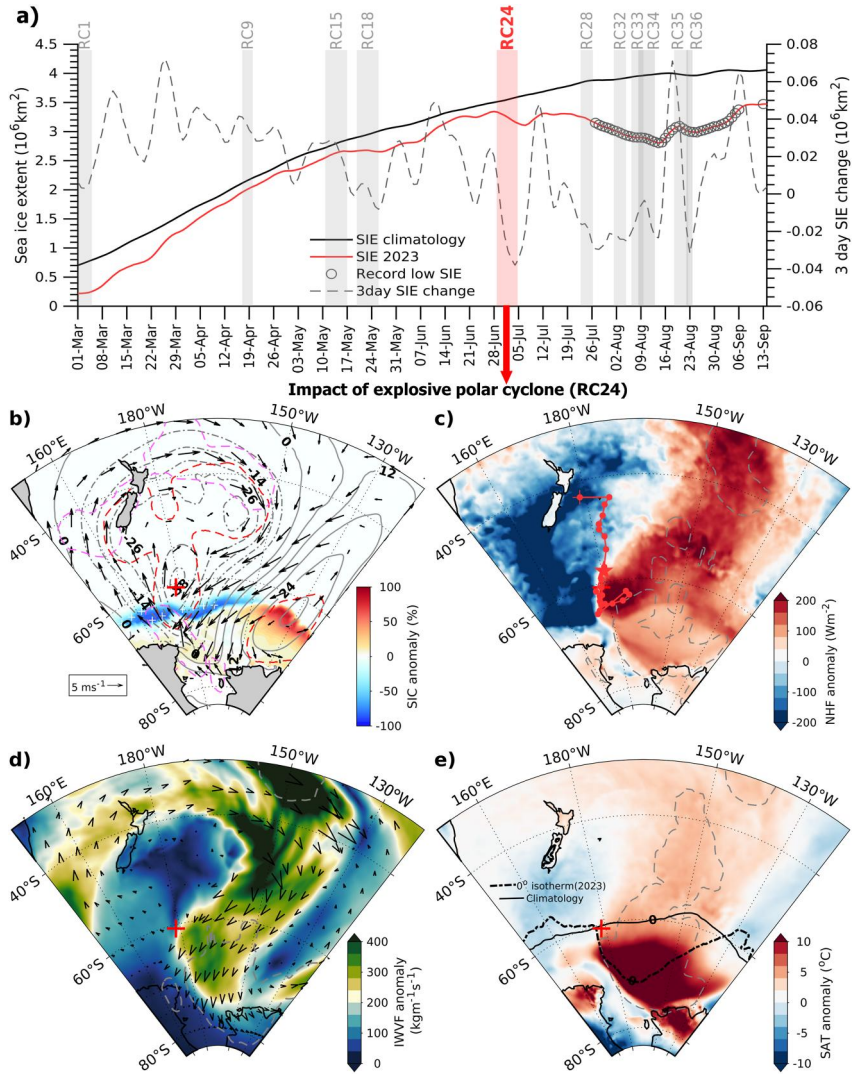

Figure 3. As Figure 2, but for the Ross Sea (160°E−130°W), and for the largest sea ice extent retreat on 01 July 2023, following the development of an explosive cyclone (RC24).

addition, an anomalous MLT warming (~2.6°C) was observed near the region of ice-edge retreat. Along with the ocean–atmosphere warming, the strong northerly wind triggered an unprecedented ice-edge retreat of 323 km from July to August 2023 to a position more than 600 km south of the climatological ice-edge (Figure 1c). Further 3-day retreat events (23.4–31.7 × 10^3 km^2) occurred on 5, 14, and 23 August, corresponding to the passage of five polar cyclones, RC32–RC36 (Figure 3a).

During the 2023 ice growth period, the region experienced 36 cyclones. The Ross Sea August SIE was a record low (2.97 × 10^6 km^2), and contributed dominantly (47.2%) to the total negative anomaly of the Southern Ocean, ahead of the annual maximum (Figure S3 in Supporting Information S1).

5. Conclusions

Ahead of the annual maximum 2023 SIE, the circumpolar ice-edge remained southward of the long-term mean, except for ice expansion in the Amundsen Sea. By August, there was positive SIC anomaly throughout much of the ABS sector that expanded more than just the Amundsen Sea. The Antarctic SIE reached a new record low level with dominant contributions of negative anomalies from the Weddell Sea during April–July, and from the Ross Sea in August–September. Although excessive upper-ocean heat was likely to be one of the factors reducing the ice expansion in 2023, the atmospheric circulation anomalies were considerable and played an important role.

The findings suggest the extremely deep ASL and its eastward shift resulted in strong northerly flow with record meridional wind anomalies across the Weddell Sea in autumn. The northerly wind gave record atmospheric temperatures and forced the ice-edge to remain southward of its mean position. Climatologically, the rate of ice growth is at maximum in May; however, a large reduction in ice growth rate during May 2023 contributed to an exceptionally low SIE in this critical period. Episodes of slow ice expansion or even ice retreats occurred during the passage of several polar cyclones, with a very large retreat in June following the development of a poleward-moving quasi-stationary cyclone with an extreme atmospheric river. In the Ross Sea, rapid changes in SIE occurred mainly in July and August 2023, corresponding to the eastward shift and record strengthening of an atmospheric block that gave record strong northerly winds off the Ross Ice Shelf. Several cyclones were again associated with periods of changing sea ice conditions; the most rapid ice retreat occurred following the passage of a poleward-moving quasi-stationary explosive cyclone in July.

The Ross and Weddell Seas SIE remained exceptionally low in September 2023, following a developing El Niño and negative SAM in winter (Figures S11a, S11c, and S11e in Supporting Information S1). From 1979 to 2022, there was low SIE in September for both the sectors without a combination of El Niño/negative SAM in the preceding months (Figure S11b–S11e in Supporting Information S1). Therefore, the regional circulation anomalies and the impact of polar cyclones are crucial (Turner et al., 2022) to explain such an unprecedented low SIE in 2023. Considering the relatively short records of satellite observations (~45 years), it is difficult to assess whether the decrease in SIE observed during the past seven years and current reduction in ice growth is part of a long-term decline as projected by climate models. While natural climate variability plays a significant role in the recent decrease in SIE (Polvani & Smith, 2013; Turner et al., 2017), the effect of anthropogenic factors may also be important (Eayrs et al., 2021; Swart et al., 2018; Wang et al., 2019) in triggering such an anomalous event. The interaction between anthropogenic forcing and internal variability is unclear within the region which needs further investigation. A comprehensive ocean-ice-atmosphere modeling is required to quantify the influence of physical drivers on rapid ice loss events and to aid predicting future climate scenarios and their potential impacts.

Data Availability Statement

We utilized the observations of sea ice concentration and sea ice extent from the passive microwave satellite sensors that provided consistent and reliable data from 1979, with a spatial resolution of 25 km × 25 km (Fetterer et al., 2017; Meier et al., 2021). The ECMWF ERA5 hourly fields are available from the Copernicus Climate Data Store (Hersbach et al., 2023). Ocean temperature and salinity data at a grid spacing of 0.25° × 0.25° was used from ECMWF ORAS5 (C3S Climate Data Store, 2021; Zuo et al., 2019). Also, we used the SAM index (Marshall, 2003) and Niño 3.4 anomalies (Rayner et al., 2003) in this paper. The input data on sea ice, SAM index, ENSO index, ASL for generating the plots (Figures 2 and 3 and Figure S11 in Supporting Information S1) is available at the open repository (Jena, 2023).

Acknowledgments

We extend our gratitude to the Director of the National Centre for Polar and Ocean Research for providing support. The Ministry of Earth Sciences, Government of India, is acknowledged for funding support. Kshitija S. acknowledges the MoES Research Fellow Program. C. Holmes and J. Wilkinson received funding under Natural Environment Research Council large Grant DEFIANT NE/W004747/1. We appreciate the data contributions from multiple sources, including the National Snow and Ice Data Center, European Centre for Medium-range Weather Forecast, National Aeronautics and Space Administration, National Oceanic and Atmospheric Administration, and their dedicated processing teams, who made various data sets available through their portals. This is NCPOR contribution number J-70/2023-24.

References

Bintanja, R., Van Oldenborgh, G. J., Drijfhout, S. S., Wouters, B., & Katsman, C. A. (2013). Important role for ocean warming and increased ice-shelf melt in Antarctic sea-ice expansion. *Nature Geoscience*, *6*(5), 376–379. https://doi.org/10.1038/ngeo1767

C3S Climate Data Store. (2021). ORAS5 global ocean reanalysis monthly data from 1958 to present [Dataset]. https://doi.org/10.24381/cds.67e8eeb7

Campbell, E. C., Wilson, E. A., Moore, G. W. K., Riser, S. C., Brayton, C. E., Mazloff, M. R., & Talley, L. D. (2019). Antarctic offshore polynyas linked to Southern Hemisphere climate anomalies. *Nature*, *570*(7761), 319–325. https://doi.org/10.1038/s41586-019-1294-0

Doddridge, E. W., & Marshall, J. (2017). Modulation of the seasonal cycle of Antarctic sea ice extent related to the southern annular mode. *Geophysical Research Letters*, *44*(19), 9761–9768. https://doi.org/10.1002/2017GL074319

Eayrs, C., Li, X., Raphael, M. N., & Holland, D. M. (2021). Rapid decline in Antarctic sea ice in recent years hints at future change. *Nature Geoscience*, *14*(7), 460–464. https://doi.org/10.1038/s41561-021-00768-3

Emanuelsson, B. D., Bertler, N. A. N., Neff, P. D., Renwick, J. A., Markle, B. R., Baisden, W. T., & Keller, E. D. (2018). The role of Amundsen–Bellingshausen Sea anticyclonic circulation in forcing marine air intrusions into West Antarctica. *Climate Dynamics*, *51*(9–10), 3579–3596. https://doi.org/10.1007/s00382-018-4097-3

Fetterer, F., Knowles, K., Meier, W. N., Savoie, M., & Windnagel, A. K. (2017). Sea ice index, version 3 [Dataset]. Average daily sea ice extent and area, using 5-day trailing averages, in square kilometers, by region of the Antarctic Ocean. National Snow and Ice Data Center, Boulder, Colorado USA. https://doi.org/10.7265/N5K072F8

Fogt, R. L., Sleinkofer, A. M., Raphael, M. N., & Handcock, M. S. (2022). A regime shift in seasonal total Antarctic sea ice extent in the twentieth century. *Nature Climate Change*, *12*(1), 54–62. https://doi.org/10.1038/s41558-021-01254-9

Francis, D., Mattingly, K. S., Temimi, M., Massom, R., & Heil, P. (2020). On the crucial role of atmospheric rivers in the two major Weddell Polynya events in 1973 and 2017 in Antarctica. *Science Advances*, *6*(46), eabc2695. https://doi.org/10.1126/sciadv.abc2695

Gilbert, E., & Holmes, C. (2024). 2023's Antarctic sea ice extent is the lowest on record. *Weather*, *79*(2), 46–51. https://doi.org/10.1002/wea.4518

Haumann, F. A., Gruber, N., Münnich, M., Frenger, I., & Kern, S. (2016). Sea-ice transport driving Southern Ocean salinity and its recent trends. *Nature*, *537*(7618), 89–92. https://doi.org/10.1038/nature19101

Hersbach, H., Bell, B., Berrisford, P., Biavati, G., Horányi, A., Sabater, J. M., et al. (2023). ERA5 hourly data on single levels from 1940 to present. Copernicus Climate Change Service (C3S) Climate Data Store (CDS) [Dataset]. https://doi.org/10.24381/cds.adbb2d47

Holland, M. M., Landrum, L., Raphael, M., & Stammerjohn, S. (2017). Springtime winds drive Ross Sea ice variability and change in the following autumn. *Nature Communications*, *8*(1), 731. https://doi.org/10.1038/s41467-017-00820-0

Hosking, J. S., Orr, A., Marshall, G. J., Turner, J., & Phillips, T. (2013). The influence of the Amundsen-Bellingshausen seas low on the climate of West Antarctica and its representation in coupled climate model simulations. *Journal of Climate*, *26*(17), 6633–6648. https://doi.org/10.1175/JCLI-D-12-00813.1

Jena, B. (2023). Southern Ocean Sea Ice data for 2023, 3-day SIE change, Amundsen Sea Low, zonal wave 3. *Mendeley Data*. V1. https://doi.org/10.17632/kjs3wch7v2.1

Jena, B., Bajish, C. C., Turner, J., Ravichandran, M., Anilkumar, N., & Kshitija, S. (2022). Record low sea ice extent in the Weddell Sea, Antarctica in April/May 2019 driven by intense and explosive polar cyclones. *Npj Climate and Atmospheric Science*, *5*(1), 19. https://doi.org/10.1038/s41612-022-00243-9

Kaufman, D. E., Friedrichs, M. A. M., Smith, W. O., Queste, B. Y., & Heywood, K. J. (2014). Biogeochemical variability in the southern Ross Sea as observed by a glider deployment. *Deep Sea Research Part I: Oceanographic Research Papers*, *92*, 93–106. https://doi.org/10.1016/j.dsr.2014.06.011

Li, X., Cai, W., Meehl, G. A., Chen, D., Yuan, X., Raphael, M., et al. (2021). Tropical teleconnection impacts on Antarctic climate changes. *Nature Reviews Earth & Environment*, *2*(10), 680–698. https://doi.org/10.1038/s43017-021-00204-5

Marshall, G. J. (2003). Trends in the Southern Annular Mode from observations and reanalyses. *Journal of Climate*, *16*(24), 4134–4143. https://doi.org/10.1175/1520-0442(2003)016<4134:TITSAM>2.0.CO;2

Martinson, D. G., & Wamser, C. (1990). Ice drift and momentum exchange in winter Antarctic pack ice. *Journal of Geophysical Research*, *95*(C2), 1741–1755. https://doi.org/10.1029/JC095iC02p01741

Meier, W. N., Stewart, J. S., Wilcox, H., Hardman, M. A., & Scott, D. J. (2021). Near-real-time DMSP SSMIS daily polar Gridded sea ice concentrations, version 2 [Dataset]. Boulder, Colorado USA. NASA National Snow and Ice Data Center Distributed Active Archive Center. https://doi.org/10.7265/tgam-yv28

Polvani, L. M., & Smith, K. L. (2013). Can natural variability explain observed Antarctic sea ice trends? New modeling evidence from CMIP5. *Geophysical Research Letters*, *40*(12), 3195–3199. https://doi.org/10.1002/grl.50578

Purich, A., & Doddridge, E. W. (2023). Record low Antarctic sea ice coverage indicates a new sea ice state. *Communications Earth and Environment*, *4*(1), 1–9. https://doi.org/10.1038/s43247-023-00961-9

Purich, A., Doddridge, E. W., Turner, J., Holmes, C., Caton Harrison, T., Phillips, T., et al. (2022). Record low Antarctic sea ice coverage indicates a new sea ice state. *Geophysical Research Letters*, *49*(12), 1–9. https://doi.org/10.1038/s43247-023-00961-9

Rayner, N. A., Parker, D. E., Horton, E. B., Folland, C. K., Alexander, L. V., Rowell, D. P., et al. (2003). Global analyses of sea surface temperature, sea ice, and night marine air temperature since the late nineteenth century. *Journal of Geophysical Research*, *108*(14). https://doi.org/10.1029/2002jd002670

Schlosser, E., Alexander Haumann, F., & Raphael, M. N. (2018). Atmospheric influences on the anomalous 2016 Antarctic sea ice decay. *The Cryosphere*, *12*(3), 1103–1119. https://doi.org/10.5194/tc-12-1103-2018

Schroeter, S., O'Kane, T. J., & Sandery, P. A. (2023). Antarctic sea ice regime shift associated with decreasing zonal symmetry in the Southern Annular Mode. *The Cryosphere*, *17*(2), 701–717. https://doi.org/10.5194/tc-17-701-2023

Stuecker, M. F., Bitz, C. M., & Armour, K. C. (2017). Conditions leading to the unprecedented low Antarctic sea ice extent during the 2016 austral spring season. *Geophysical Research Letters*, *44*(17), 9008–9019. https://doi.org/10.1002/2017GL074691

Swart, N. C., Gille, S. T., Fyfe, J. C., & Gillett, N. P. (2018). Recent Southern Ocean warming and freshening driven by greenhouse gas emissions and ozone depletion. *Nature Geoscience*, *11*(11), 836–841. https://doi.org/10.1038/s41561-018-0226-1

Turner, J., Holmes, C., Caton Harrison, T., Phillips, T., Jena, B., Reeves-Francois, T., et al. (2022). Record low Antarctic sea ice cover in February 2022. *Geophysical Research Letters*, *49*(12), e2022GL098904. https://doi.org/10.1029/2022GL098904

Turner, J., Hosking, J. S., Bracegirdle, T. J., Marshall, G. J., & Phillips, T. (2015). Recent changes in Antarctic sea ice. *Philosophical Transactions of the Royal Society A: Mathematical, Physical & Engineering Sciences*, *373*(2045), 20140163. https://doi.org/10.1098/rsta.2014.0163

Turner, J., Phillips, T., Marshall, G. J., Hosking, J. S., Pope, J. O., Bracegirdle, T. J., & Deb, P. (2017). Unprecedented springtime retreat of Antarctic sea ice in 2016. *Geophysical Research Letters*, *44*(13), 6868–6875. https://doi.org/10.1002/2017GL073656

Vichi, M., Eayrs, C., Alberello, A., Bekker, A., Bennetts, L., Holland, D., et al. (2019). Effects of an explosive polar cyclone crossing the Antarctic marginal ice zone. *Geophysical Research Letters*, *46*(11), 5948–5958. https://doi.org/10.1029/2019GL082457

Wang, G., Hendon, H. H., Arblaster, J. M., Lim, E.-P., Abhik, S., & van Rensch, P. (2019). Compounding tropical and stratospheric forcing of the record low Antarctic sea-ice in 2016. *Nature Communications*, *10*(1), 13. https://doi.org/10.1038/s41467-018-07689-7

Xia, B. L., Zahn, M., Hodges, K. I., Feser, F., & Storch, H. V. (2012). A comparison of two identification and tracking methods for polar lows. *Tellus, Series A: Dynamic Meteorology and Oceanography*, *64*(1), 17196. https://doi.org/10.3402/tellusa.v64i0.17196

Zuo, H., Balmaseda, M. A., Tietsche, S., Mogensen, K., & Mayer, M. (2019). The ECMWF operational ensemble reanalysis-analysis system for ocean and sea ice: A description of the system and assessment. *Ocean Science*, *15*(3), 779–808. https://doi.org/10.5194/os-15-779-2019